Loyola University Chicago
Loyola eCommons

Chemistry: Faculty Publications and Other Works

Faculty Publications and Other Works by Department

2006

Controlling Charge Injection in Organic Field-Effect Transistors Using Self-Assembled Monolayers

B H. Hamadani

D A. Corley

Jacob W. Ciszek
Loyola University Chicago, jciszek@luc.edu

J M. Tour

D Natelson

Follow this and additional works at: https://ecommons.luc.edu/chemistry_facpubs

Part of the Chemistry Commons

Recommended Citation

Hamadani, BH, DA Corley, JW Ciszek, JM Tour, and D Natelson. "Controlling charge injection in organic field-effect transistors using self-assembled monolayers" in Nano Letters 6(6) 2006. http://dx.doi.org/10.1021/nl060731i

This Article is brought to you for free and open access by the Faculty Publications and Other Works by Department at Loyola eCommons. It has been accepted for inclusion in Chemistry: Faculty Publications and Other Works by an authorized administrator of Loyola eCommons. For more information, please contact ecommons@luc.edu.

This work is licensed under a Creative Commons Attribution-Noncommercial-No Derivative Works 3.0 License.
© 2006 American Chemical Society.

Controlling charge injection in organic field-effect transistors using self-assembled monolayers

B. H. Hamadani[1], D. A. Corley[2], J. W. Ciszek[2], J. M. Tour[2] and D. Natelson*[1,3]
[1] *Department of Physics and Astronomy, Rice University*
[2] *Department of Chemistry and Smalley Institute for Nanoscale Science and Technology, Rice University and*
[3] *Department of Electrical and Computer Engineering,*
Rice University, 6100 Main St., Houston, TX 77005

arXiv:cond-mat/0605605v1 [cond-mat.mtrl-sci] 24 May 2006

We have studied charge injection across the metal/organic semiconductor interface in bottom-contact poly(3-hexylthiophene) (P3HT) field-effect transistors, with Au source and drain electrodes modified by self-assembled monolayers (SAMs) prior to active polymer deposition. By using the SAM to engineer the effective Au work function, we markedly affect the charge injection process. We systematically examine the contact resistivity and intrinsic channel mobility, and show that chemically increasing the injecting electrode work function significantly improves hole injection relative to untreated Au electrodes.

Improved understanding of the dynamics of charge motion at interfaces between metals and organic semiconductors (OSCs) is crucial for optimizing the performance of organic optoelectronic devices, including organic field-effect transistors (OFETs). In an OFET the electronic structure of the OSC/contacting electrode interface can strongly affect the overall performance of the device. The band alignment at the OSC/metal interface is influenced by several factors such as interfacial dipole formation[1, 2, 3], electrode contamination[4], and OSC doping[5, 6, 7]. Depending on the particular band alignment, the charge injection mechanism can significantly change, as seen by *e.g.* linear (ohmic) or nonlinear current-voltage characteristics.

Ohmic contacts between metals and inorganic semiconductors are often achieved by strong local doping of the contact regions, but such an approach is challenging to implement in OSCs. Bulk doping levels in the OSC do affect injection. In recent work[7] examining charge injection in bottom-contact OFETs based on poly(3-hexylthiophene) (P3HT), we found that large contact resistances and nonlinear transport at low dopant concentrations are consistent with the formation of an increased injection barrier for holes. Band alignment is also significant[8]. For example[7], the onset of nonohmic transport at low doping is much more severe in devices with Au source and drain electrodes than Pt. It has previously been shown[9, 10, 11, 12] that, by self-assembly of a layer of molecules with an intrinsic electric dipole moment, the work function of metal electrodes can be lowered or raised, affecting the size of the injection barrier at the metal/OSC interface. While limited attempts have been made to use this approach to engineer contacts in OFETs[13, 14], considerably more effort has been dedicated to contacts in organic light emitting diodes (OLEDs)[10, 11, 17] and modification of the OSC/dielectric interface[15, 16] in OFETs. In contrast to OLEDs, OFETs allow studies of transport with a single carrier type, with carrier density tunable independently of the source-drain bias, and with established procedures for discerning between contact and bulk effects. Minimizing contact resistances is particularly challenging in planar OFETs since active contact areas are generally much smaller than in vertical OLEDs.

In this letter, using channels of varying length, we systematically examine the contact resistances and true channel mobility at various doping levels of bottom-contact P3HT OFETs with Au electrodes modified by self-assembly of dipolar molecular monolayers. We correlate the transport data with self-assembled monolayer (SAM) induced work function changes as measured by scanning potentiometry. In the case of electron-poor (work function-raising) SAMs, we show that contact resistances remain low compared to the channel resistance and the transistors show linear transport. These observations are consistent with the "pinning" of the local chemical potential at the interface at an energy favorable to hole injection, and contrast sharply with the strongly nonlinear injection observed at low doping levels in OFETs made with bare Au electrodes. Furthermore, devices with electrodes modified by electron rich (work function-lowering) SAMs show nonlinear transport and low currents at all doping levels, becoming increasingly nonlinear as dopant density is reduced. This is consistent with formation of an increased injection barrier for holes in such devices.

OFETs are made in a bottom-contact configuration[18] on a degenerately doped $p+$ silicon wafer used as a gate. The gate dielectric is 200 nm of thermal SiO_2. Source and drain electrodes are patterned using electron beam lithography in the form of an interdigitated set of electrodes with systematic increase in the distance between each pair. The channel width, W, is kept fixed for all devices at 200 μm. The electrodes are deposited by electron beam evaporation of 2.5 nm of Ti and 25 nm of Au, followed by lift off. This thickness of metal is sufficient to guarantee film continuity and good metallic conduction while attempting to minimize disruptions of the surface topography that could adversely affect polymer morphology.

Prior to SAM assembly, the substrates were cleaned for 2 min in an oxygen plasma. They were then immersed

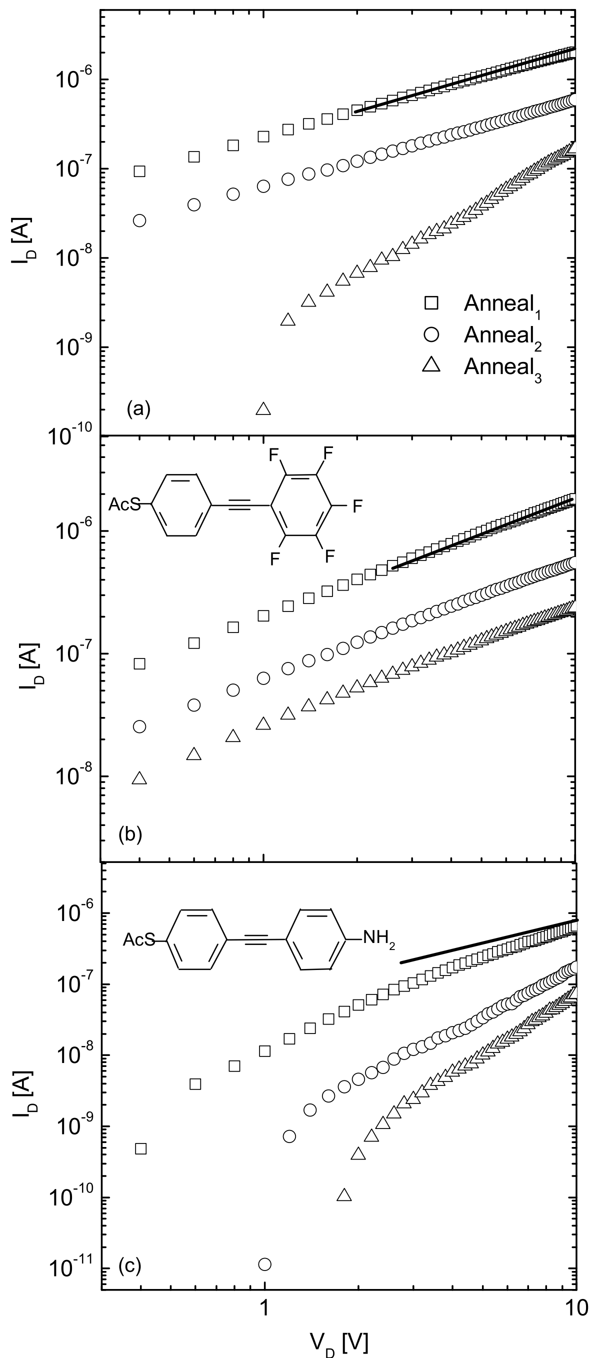

FIG. 1: (a) A log-log plot of the transport characteristics of a Au/P3HT device for different annealing as described in the text. (b) Similar plot for a Au/P3HT device with the electrodes modified by F-OPE SAM shown in the inset. (c) Au/P3HT device with electrodes modified by OPE-NH_2 SAM molecules shown in the inset. For all devices, $L = 40$ μm at $T = 300$ K and at a fixed $V_G = -70$ V with the same annealing schedule. The solid black line has a slope of 1.

for about 24 h in a 1:1 ethanol-chloroform solution of the desired molecule at a $\sim$0.25 mg/mL concentration, prepared under nitrogen gas. Three types of molecules were used in this experiment: an electron poor fluorinated oligo(phenylene ethynylene) (F-OPE) (see Fig. 1b inset), and two electron-rich oligomers, OPE-NH_2 (Fig 1c inset) and OPE-2(NH_2) (not shown, but similar to OPE-NH_2 with an additional amine group immediately adjacent to the first). These molecules self-assemble from the thioacetate through standard Au-thiol deprotection chemistry[19], and their characterization are described in detail in the supplementary online material. F-OPE molecules are electron poor and upon assembly boost the metal work function (*vide infra*), while the amine-terminated OPEs are electron rich and are expected to have the opposite effect.

To characterize the effect of the SAM molecules on the effective Au work function, we used a multi-mode atomic force microscope (AFM) in the surface potential mode[22] to measure the surface potential difference between the SAM treated and bare Au substrates. While not suited to absolute measurements of work function, this method is useful for comparing relative differences in work function between differently treated surfaces. By comparing measured contact potentials of unmodified and SAM-coated Au films, we found that the F-OPE treated Au substrates exhibited an effective work function increased by $\sim$0.9 eV for an assembly period of two days relative to untreated co-evaporated Au films. In addition, the F-OPE treated samples showed stability and consistency in contact potential measurements over extended periods (days) of exposure to ambient conditions. For the OPE-NH_2 and OPE-2(NH_2) treated surfaces, however, it was difficult to obtain consistent surface potential differences with respect to bare Au, though most showed a slight decrease ($\sim$0.1 eV) in work function. These difficulties appear to result from instability of the resulting surfaces under extended exposure to ambient conditions. However, as shown below, these electron-rich molecules have a clear impact on band energetics at the interface, with transport measurements suggesting the formation of an injection barrier for holes.

The organic semiconductor, 98% regio-regular P3HT [20], is dissolved in chloroform at a 0.06% weight concentration, passed through polytetrafluoroethylene (PTFE) 0.2 μm filters and solution cast onto the treated substrate, with the solvent allowed to evaporate in ambient conditions. The resulting films are tens of nm thick as determined by atomic force microscopy. The measurements are performed in vacuum ($\sim 10^{-6}$ Torr) in a variable temperature range probe station using a semiconductor parameter analyzer. Exposure to air and humidity is known to enhance hole doping in P3HT[21]. To reduce this impurity doping, the sample is annealed at elevated temperatures ($\sim$350-380 K) in vacuum for several hours and then cooled to room temperature for measurement. This results in a reduction in the background dopant concentration as easily characterized through the two-terminal bulk P3HT conductivity.

The devices operate as standard *p*-type FETs in ac-

cumulation mode. With the source electrode grounded, the devices are measured in the shallow channel regime ($V_D < V_G$). Figure 1(a) shows the transport characteristics of a Au/P3HT device with $L = 40$ μm at $T = 300$ K and at a fixed $V_G = -70$ V for different doping levels. In anneal$_1$, the sample was vacuum treated in the analysis chamber at 300 K for 16 h. Anneal$_2$ corresponds to the sample being further heated in vacuum for 18 h at 350 K, while anneal$_3$ includes yet an additional 18 h at 360 K. As in earlier experiments[7], the transport in this device with unmodified Au electrodes becomes nonlinear at high annealing steps, and the current drops by orders of magnitude. We attributed this to the formation of an increased injection barrier for holes, and similar effects have been reported by others[23].

In contrast, Fig. 1(b) shows the transport for a device with similar geometric parameters and annealing schedule, in which the electrodes were modified by F-OPE SAM molecules prior to P3HT deposition. Even though I_D drops at higher annealing steps, the currents remain linear with V_D and as shown below, the contact resistance remains much lower compared to bare Au devices. This behavior is similar to our previous observations[7] for Pt/P3HT devices. These effects have been verified in annealing cycles on multiple arrays of F-OPE treated devices.

In Fig. 1(c), the electrode surfaces were modified by OPE-NH_2. In this case, the currents are much lower than in either (a) or (b), and even when the hole doping of the P3HT is significant, injection is nonohmic, with I_D rising super-linearly with V_D. In highly annealed conditions, this behavior is super-quadratic. Transport data for the OPE-2(NH_2) treated devices qualitatively looks very similar to those in Fig. 1(c).

From the data in Figs. 1(a) and 1(b), we extracted the channel resistance, R_{ch}, the intrinsic device mobility, μ, and the contact resistance R_c from the L dependence of the total device resistance, $R_{on} \equiv \partial V_D/\partial I_D$ over a T and V_G range as described in Ref.[18]. We obtain R_c in the limit $|V_D| < 1V$, where transport is still reasonably linear even after the longer annealing runs. We note that while we have developed a procedure for extracting contact current-voltage characteristics even in the limit of strong injection nonlinearities[8], it is difficult to quantify such injection by a single number such as R_c. In the shallow channel limit, it is straightforward to convert the gate dependence of R_{ch} into a field-effect mobility[18].

Figure 2(a) shows a log-log plot of μ vs R_c for two sets of devices over a series of temperatures and gate voltages for an initial annealing step. The open symbols correspond to data from the F-OPE treated electrodes and the filled symbols are extracted from bare Au/P3HT data. The error bars come from the uncertainty in the slope and intercept of R_{on} vs. L plots[18]. Indeed, in device arrays with $R_c << R_{ch}$, deviations from perfect scaling of $R_{ch} \propto L$ can lead to "best fit" values of R_c that are actually negative (and hence cannot be plotted on such a figure), though with appropriately large error bars. Here,

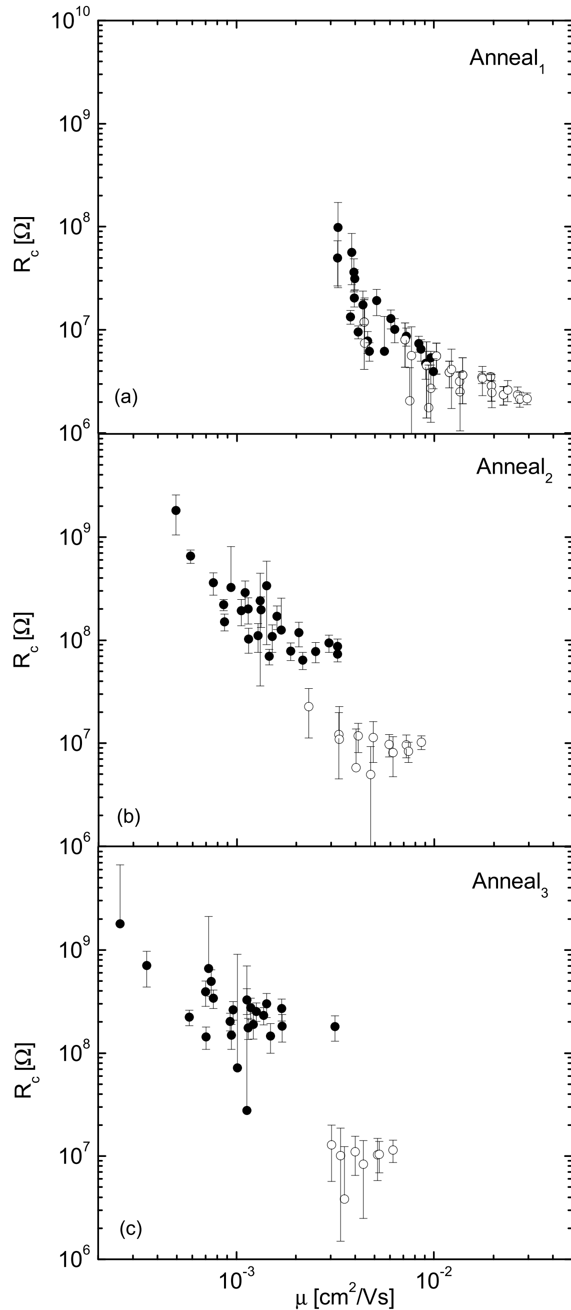

FIG. 2: (a) A log-log plot of μ vs R_c for 2 sets of devices over a series of temperatures and gate voltages. The open symbols correspond to data from the F-OPE treated electrodes and the filled symbols are extracted from bare Au/P3HT data. Anneal$_1$ here corresponds to sample being pumped on in vacuum at 320 K overnight (b) data retaken after sampled was annealed at 350 K for 18 h (anneal$_2$) (c) data taken again after another anneal step similar to (b). The reason for fewer data points in Fig. (b) and Fig. (c) for SAM treated sample is a smaller contact resistance with significant error compared to the channel resistance.

the mobility and the contact resistance for both device

sets are similar, consistent with similarity in the magnitude of $I_D - V_D$ for both samples. In the proceeding annealing steps, however, the contact resistance for the sample with untreated electrodes increases significantly, compared to the SAM treated device (Figs. 2(b) and (c)). Whereas the Au/P3HT devices become severely contact limited at high dedopings, the treatment of Au electrodes with F-OPE molecules keeps the contact resistance relatively low compared to channel resistance, and the transport characteristics remain *linear*. This ohmic injection persists even when bulk $V_G = 0$ conduction in the P3HT film is completely suppressed at room temperature.

Our results in F-OPE treated devices are quantitatively similar to those obtained in charge injection from Pt electrodes into P3HT[7]. Although it is difficult to probe the energy level alignment directly at the metal/organic interface (due to the the thick P3HT film resulting from solution casting), it is clear that increasing the Au effective work function results in improved electronic performance of these OFETs. In light of the many experiments showing the formation of interfacial dipoles at the metal/OSC interface upon deposition of the OSC[1, 2, 3], it is possible that introduction of workfuction-raising SAMs such as F-OPE in our experiments counteracts or prevents the work function-lowering effect of these interfacial dipoles. This can result in a "pinning" of the energy levels at the interface such that there is a small or non-existent injection barrier for holes. On the other hand, the work function-lowering OPE-NH_2 SAMs appear to contribute more substantially to the interfacial dipoles, resulting in significant Schottky barrier formation for holes at the interface and severe nonlinear injection in these devices. The subsequent dedopings have the same implications discussed earlier[7].

One must also consider whether the different injection properties could result from SAM-induced changes in the ordering of the P3HT at the metal-OSC interface. Such morphological differences may occur, and would require careful interface-sensitive spectroscopies or scattering measurements to confirm. However, while improved P3HT ordering at the F-OPE/P3HT interface would result in higher mobilities and lower contact resistances, we find it unlikely that morphological changes alone could explain the dramatic difference in injection properties as a function of doping. The data in Fig. 2 strongly suggest significant differences in the band energetics between the F-OPE treated and untreated Au electrodes.

We have used dipole-containing self-assembled monolayers on the Au source and drain electrodes to strongly manipulate the charge injection process across the metal-organic interface in a series of polymer FETs based on P3HT. To see the effect of dopant concentration on device performance, we measure device properties after each of a series of mild annealing steps in vacuum. We extract the contact resistances and the intrinsic channel mobility from the length dependence of the resistance for bare Au/P3HT and flourinated-OPE Au/P3HT devices where transport is still relatively linear at low drain bias. At low dopant concentrations, SAM-modified devices show significantly lower contact resistances and higher mobilities compared to unmodified devices. We attribute these findings to higher metal work function and small injection barriers for holes in the case of F-OPE SAM modified devices, resulting from better energetic alignment with the valence band of the organic semiconductor. These results quantitatively demonstrate the power of simple surface chemistry in modifying the dynamics of charge at interfaces with OSCs, even in nearly undoped material. Such techniques will be generally useful in significantly improving technologies based on these versatile materials.

D.N. acknowledges support from the David and Lucille Packard Foundation, the Alfred P. Sloan Foundation, the Robert A. Welch Foundation, and the Research Corporation. J.M.T. acknowledges support from DARPA and AFOSR.

---

[1] Watkins, N. J.; Yan, L.; Gao, Y. *Appl. Phys. Lett.* **2002**, *80*, 4384-4386.
[2] Knupfer, M.; Paasch, G. *J. Vac. Sci. Technol. A* **2005**, *23*, 1072-1077.
[3] Ishii, H.; Sugiyama, K.; Ito, E.; Seki, K. *Adv. Mater.* **1999**, *11*, 605-625.
[4] Wan, A.; Hwang, J.; Amy, F.; Kahn, A. *Org. Elec.* **2005**, *6*, 47-54.
[5] Gao, W.; Kahn, A. *Appl. Phys. Lett.* **2001**, *79*, 4040-4042.
[6] Gao, W.; Kahn, A. *J. Appl. Phys.* **2003**, *94*, 359-366.
[7] Hamadani, B. H.; Ding, H.; Gao, Y.; Natelson, D. *Phys. Rev. B* **2005**, *72*, 235302.
[8] Hamadani, B. H.; Natelson, D. *J. Appl. Phys.* **2005**, *97*, 064508.
[9] Campbell, I. H.; Rubin, S.; Zawodzinski, T. A.; Kress, J. D.; Martin, R. L.; Smith, D. L.; Barashkov, N. N.; Ferraris, J. P. *Phys. Rev. B* **1996**, *54*, R14321-R14324.
[10] Nüesch, F.; Rotzinger, F.; Si-Ahmed, L.; Zuppiroli, L. *Chem. Phys. Lett.* **1998**, *288*, 861-867.
[11] Zuppiroli, L.; Si-Ahmed, L.; Kamaras, K.; Nüesch, F.; Bussac, M.N.; Ades, D.; Siove, A.; Moons, E.; Grätzel, M. *Eur. J. Phys. B* **1999**, *11*, 505-512.
[12] Tour, J. M.; Rawlett, A. M.; Kozaki, M.; Yao, Y.; Jagessar, R. C.; Dirk, S. M.; Price, D. W.; Reed, M. A.; Zhou, C.-W.; Chen, J.; Wang, W.; Campbell, I. H. *Chem. Eur. J.* **2001**, *7*, 5118-5134.
[13] Gundlach, D. J.; Jia, L.; Jackson, T. N. *IEEE Elec. Dev. Lett.* **2001**, *22*, 571-573.
[14] Kim, S. H.; Lee, J. H.; Lim, S. C.; Yang, Y. S.; Zyung, T.; *Jpn. J. Appl. Phys.* **2003**, *43*, L60-L62.
[15] Pernstich, K. P.; Haas, S.; Oberhoff, D.; Goldmann, C.; Gundlach, D. J.; Batlogg, B.; Rashid, A. N.; Schitter, G. *J. Appl. Phys.* **2004**, *96*, 6431-6438.

[16] Kline, R.J.; McGehee, M.D.; Toney, M.F. *Nat. Mater.* **2006**, *5*, 222-228.

[17] de Boer, B.; Hadipour, A.; Mandoc, M. M.; van Woudenbergh, T.; Blom, P. W. M. *Adv. Mater.* **2005**, *17*, 621-625.

[18] Hamadani, B. H.; Natelson, D. *Appl. Phys. Lett.* **2004**, *84*, 443-445.

[19] Cai, L.; Yao, Y.; Yang, J.; Price, D. W., Jr.; Tour, J. M. *Chem. Mater.* **2002**, *14*, 2905-2909.

[20] Sigma-Aldrich Inc., St. Louis, MO.

[21] Hoshino, H.; Yoshida, M.; Uemura, S.; Kodzasa, T.; Takada, N.; Kamata, T.; and Yase, K. *J. Appl. Phys.* **2004**, *95*, 5088-5093.

[22] Surface Potential Detection manual, Veeco Inst. Sec.231.6.

[23] Rep, D. B. A.; Morpurgo, A. F.; Klapwijk, T. *Org. Elect.* **2003**, *4*, 201-207.